

VERY HIGH REDSHIFT X-RAY SELECTED AGN IN THE *CHANDRA* DEEP FIELD-NORTH

A. J. BARGER,^{1,2,3} L. L. COWIE,³ P. CAPAK,³ D. M. ALEXANDER,⁴ F. E. BAUER,⁴
 W. N. BRANDT,⁴ G. P. GARMIRE,⁴ A. E. HORNSCHMEIER^{5,6}

To appear in The Astrophysical Journal Letters

ABSTRACT

Deep *Chandra* X-ray exposures provide an efficient route for locating optically faint active galactic nuclei (AGN) at high redshifts. We use deep multicolor optical data to search for $z > 5$ AGN in the 2 Ms X-ray exposure of the *Chandra* Deep Field-North. Of the 423 X-ray sources bright enough ($z' < 25.2$) for a color-color analysis, at most one lies at $z = 5 - 6$ and none at $z > 6$. The $z > 5$ object is spectroscopically confirmed at $z = 5.19$. Only 31 of the 77 sources with $z' > 25.2$ are undetected in the *B* or *V* bands at the 2σ level and could lie at $z > 5$. There are too few moderate luminosity AGN at $z = 5 - 6.5$ to ionize the intergalactic medium.

Subject headings: cosmology: observations — galaxies: active — galaxies: evolution — galaxies: formation — galaxies: distances and redshifts

1. INTRODUCTION

Most of our current information on very high redshift active galactic nuclei (AGN) relates to the very high luminosity tail of the luminosity function (LF). At $z > 5$ the Sloan Digital Sky Survey (SDSS) probes to an 1450 Å absolute magnitude of about -26 (Fan et al. 2001a, b), much brighter than the average luminosity of AGN at lower redshifts (Pei 1995). Calculations of the contributions of high-redshift AGN to the ionizing flux in the Universe must therefore rely on large extrapolations (e.g., Madau, Haardt, & Rees 1999), and deeper observations of the LF are needed to constrain this quantity directly. Such observations can also test models of supermassive black hole formation (e.g., Haiman & Loeb 1998, 1999; Haehnelt, Natarajan, & Rees 1998).

We can efficiently search for faint, high-redshift AGN using combined ultradeep X-ray and optical imaging. Since at high redshifts observed-frame X-ray bands correspond to very high rest-frame energies, we can obtain a relatively complete sample of AGN, including sources surrounded by very high column densities of gas and dust. Some Compton-thick sources may be omitted from the sample but would not be expected to contribute much to the ionizing light. As there are only a handful of stars in X-ray samples, there is little problem in separating red stars from high-redshift AGN. Here we use deep broad-band optical imaging and follow-up optical spectroscopy to measure the $z > 5$ AGN population in the *Chandra* Deep Field-North (CDF-N) 2 Ms exposure. We assume $\Omega_M = 1/3$, $\Omega_\Lambda = 2/3$ and $H_0 = 65 \text{ km s}^{-1} \text{ Mpc}^{-1}$.

2. DATA

The deepest X-ray image is the ≈ 2 Ms CDF-N exposure centered on the Hubble Deep Field-North. D. M.

Alexander et al. (in preparation) merged samples detected in seven X-ray bands to form a catalog of 503 point sources over an area of 460 arcmin². Near the aim point the limiting fluxes are $\approx 1.5 \times 10^{-17} \text{ erg cm}^{-2} \text{ s}^{-1}$ (0.5 – 2 keV) and $\approx 10^{-16} \text{ erg cm}^{-2} \text{ s}^{-1}$ (2 – 8 keV). The sensitivity degrades with off-axis angle beyond $\sim 6'$, rising to about $10^{-15} \text{ erg cm}^{-2} \text{ s}^{-1}$ (0.5 – 2 keV) and $10^{-14} \text{ erg cm}^{-2} \text{ s}^{-1}$ (2 – 8 keV) at the maximum angle of $\sim 14'$. The 2 – 8 keV number counts and completeness levels in the 1 Ms exposure of the CDF-N are described in Cowie et al. (2002a).

Johnson *B* and *V*, Cousins *R* and *I*, and Sloan z' images were obtained on the Subaru⁷ 8.2 m telescope's Prime Focus Camera (Suprime-Cam; Miyazaki et al. 2002). The observations and reductions are summarized in P. Capak et al. (in preparation). The exposure times are z' (3.9 hrs), *I* (2.9 hrs), *R* (5.3 hrs), *V* (8.4 hrs), and *B* (1.7 hrs). The image quality is $\approx 0.8''$, except in the *V* (1.0'') and *R* (1.1'') bands. Magnitudes and images are given in Barger et al. (2002; 1 Ms sample) and A. J. Barger et al. (in preparation; 2 Ms). We chose the optical position to be the highest surface brightness peak in the z' image within $1.5''$ of the X-ray position. For most sources the optical counterpart is unambiguous, but in some cases (about 7%), there is more than one possible counterpart (see, e.g., Fig. 2 of Barger et al. 2002). We discuss alternative counterparts in § 3.2. For off-axis sources in extended galaxies, and optically faint sources, we used the X-ray position.

We measured magnitudes in $2''$ diameter apertures on images smoothed to the lowest resolution image (*R*) to provide the most accurate colors. We estimated total magnitudes by correcting the $2''$ diameter magnitudes to $6''$ diameter using a median offset (~ 0.8 for each filter) measured on the smoothed images. Three of the sources lie too close to bright stars for accurate photometry; we ex-

¹Department of Astronomy, University of Wisconsin-Madison, 475 North Charter Street, Madison, WI 53706

²Department of Physics and Astronomy, University of Hawaii, 2505 Correa Road, Honolulu, HI 96822

³Institute for Astronomy, University of Hawaii, 2680 Woodlawn Drive, Honolulu, HI 96822

⁴Department of Astronomy & Astrophysics, 525 Davey Laboratory, The Pennsylvania State University, University Park, PA 16802

⁵Chandra Fellow

⁶Department of Physics and Astronomy, Johns Hopkins University, 3400 North Charles Street, Baltimore, MD 21218

⁷The Subaru telescope is operated by the National Astronomical Observatory of Japan.

cluded these objects. We use the AB magnitude system with $m_{AB} = -2.5 \log f_\nu - 48.60$, where f_ν is the flux of the source in units of $\text{erg cm}^{-2} \text{s}^{-1} \text{Hz}^{-1}$. The 1σ limits on the total magnitudes are 28.5 (B), 28.4 (V), 28.2 (R), 27.3 (I), and 26.9 (z') based on measuring randomly positioned apertures in the field. These are slightly more conservative (brighter) than those used in Barger et al. (2002), where the limits were computed for $3''$ diameter aperture magnitudes using the distribution of sky backgrounds in the individual pixels. The present limits deal better with correlated noise.

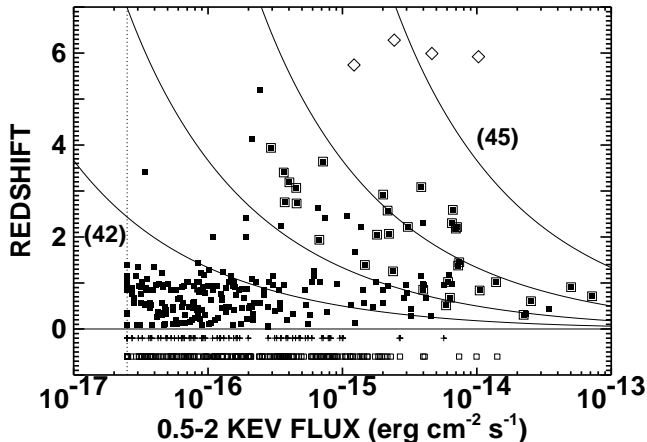


FIG. 1.— Redshift versus 0.5 – 2 keV flux for the entire sample. Sources fainter than $2.5 \times 10^{-17} \text{ erg cm}^{-2} \text{s}^{-1}$ are shown at this limit. Three sources with poor optical photometry are excluded from the plot, as are the 13 spectroscopically identified stars. Solid curves show flux versus redshift for sources with a 2 – 8 keV rest-frame luminosity of $L_x = 10^{42} \text{ erg s}^{-1}$ (lowest curve), $10^{43} \text{ erg s}^{-1}$, $10^{44} \text{ erg s}^{-1}$, and $10^{45} \text{ erg s}^{-1}$ (highest curve), computed with a K -correction for an intrinsic $\Gamma = 1.8$ power-law spectrum where Γ is the photon index. Sources with broad-line optical spectra are enclosed in a second, larger symbol. Spectroscopically unidentified sources with $z' < 25.2$ ($z' > 25.2$) are denoted by open squares (plus signs) at $z = -0.7$ ($z = -0.3$). Large open diamonds denote the optically-selected high-redshift quasars from the SDSS sample (Brandt et al. 2002; Mathur et al. 2002).

Figure 1 shows redshift versus 0.5 – 2 keV flux. Barger et al. (2002) and A. J. Barger et al. (in preparation) give optical spectroscopic identifications for 249 of the X-ray sources, including 16 off-axis sources where the X-ray position is within the envelope of a bright galaxy but not within $1.5''$ of the nucleus (Hornschemeier et al. 2002). We analyze the colors for the 423 (out of the 500 with accurate photometry) X-ray sources with optical counterparts brighter than the 5σ limit of $z' = 25.2$. In Fig. 1 we split the spectroscopically unidentified counterparts into $z' < 25.2$ (open squares at $z = -0.6$) and $z' > 25.2$ (plus signs at $z = -0.3$).

The solid curves in Fig. 1 are for fixed rest-frame 2 – 8 keV luminosities ranging from $10^{42} \text{ erg s}^{-1}$ (lowest curve) to $10^{45} \text{ erg s}^{-1}$ (highest curve). The open diamonds show the 0.5 – 2 keV fluxes of the highest redshift sources from the SDSS sample (Brandt et al. 2002; Mathur et al. 2002). These form an optically complete sample for $z > 5.7$ and $z' < 20$ over an area of 1500 deg^2 (Fan et al. 2001b). The present X-ray sample probes almost two orders of magnitude fainter than the typical X-ray flux seen in the SDSS sample; however, the area of sky cov-

ered is four orders of magnitude smaller. If the rest-frame optical to rest-frame X-ray flux ratios of high-redshift, low-luminosity sources are similar to those of the high-redshift, high-luminosity sources in the SDSS sample, then the magnitudes of the optical counterparts to the low-luminosity sources would go as faint as $z' = 25$, which is well-matched to our $z' = 25.2$ color-selection limit. However, if instead high-redshift, low-luminosity sources have lower rest-frame optical to X-ray flux ratios (Green et al. 1995; Vignali, Brandt, & Schneider 2003), then the counterparts could be fainter than $z' = 25$.

3. HIGH REDSHIFT AGN

3.1. Optically Bright Sample

High-redshift sources in the X-ray sample are easily identified because the increasing line blanketing of the Lyman forest at high redshifts produces extremely large breaks across redshifted $\text{Ly}\alpha$ (e.g., Fan et al. 2001b). Songaila & Cowie (2002) measured the average forest transmission in the redshift range $z = 3.8 - 6.2$. The magnitude break across $\text{Ly}\alpha$ is

$$\Delta m = 3.8 + 20.3 \log_{10} \left(\frac{1+z}{7} \right). \quad (1)$$

At $z = 5$, where $\text{Ly}\alpha$ lies between R and I , the break is 2.4 magnitudes, while at $z = 6$, where $\text{Ly}\alpha$ lies between I and z' , it is 3.8 magnitudes. If the epoch of reionization is at $z \sim 6.1$ (Becker et al. 2001), then the break is extremely large at redshifts higher than this. The $\text{Ly}\alpha$ line moves through our longest wavelength (z') band at $z \approx 6.5$, which is the largest redshift where a source would be seen in our optical data.

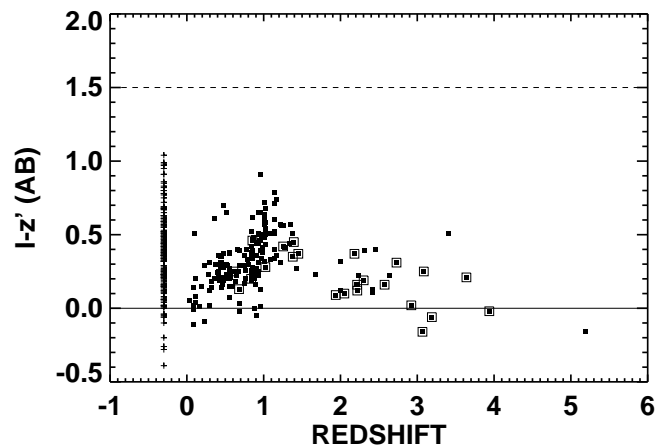


FIG. 2.— $I - z'$ in the AB system versus redshift for the 423 sources with $z' < 25.2$. Sources without redshifts are shown at $z = -0.3$, and broad-line AGN are enclosed in a second, larger symbol. The dashed line ($I - z' = 1.5$) is the color of $z \sim 6$ sources in the quasar and galaxy models described in the text. None of the spectroscopically unidentified sources are red enough in $I - z'$ to be at $z > 6$.

Figure 2 shows $I - z'$ versus redshift (spectroscopically unidentified sources are at $z = -0.3$) for our $z' < 25.2$ sample. We see from Fig. 2 that none of the sources lie at $z > 6$, since such sources would be redder than $I - z' > 1.5$. In Fig. 3 we show $V - I$ versus $I - z'$. The dashed line is the track with redshift of the composite SDSS quasar

spectrum of Vanden Berk et al. (2001), extrapolated with a $f_\nu \sim \nu^{-0.46}$ power-law below $\text{Ly}\alpha$, modulated by the Songaila & Cowie (2002) forest transmissions, and convolved through the Suprime-Cam filters. The extrapolation below the Lyman continuum limit is not critical since the high incidence of Lyman limit systems at these redshifts truncates the spectrum at shorter wavelengths. The dot-dash line shows the same calculation for a $f_\nu \sim \nu^0$ galaxy with no emission lines and a cut-off at 912 Å. The deep forest absorption moves the tracks far from the galaxy populations. Apart from the one $z = 5.19$ AGN (large solid square) with $z' = 23.9$, there are no other $z > 5$ candidates. Given the possibility that in a small number of cases we may have chosen the wrong optical counterpart or the colors are contaminated by a nearby object, we also visually searched differenced images for objects with red $V - I$ colors. No further candidates were found.

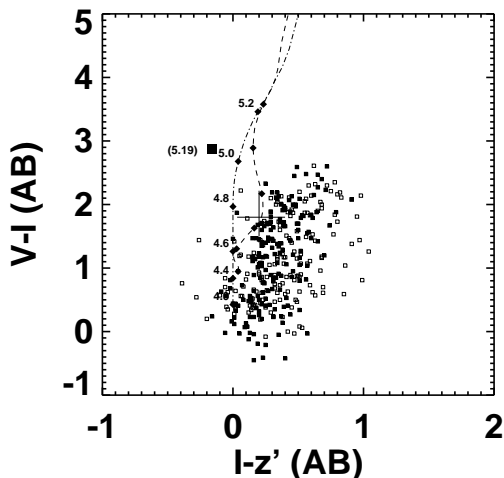


FIG. 3.— $V - I$ versus $I - z'$ for the $z' < 25.2$ sample. Solid (open) squares denote galaxies with (without) redshift identifications. All sources are detected above the 2σ level in all three bands. One sigma uncertainties are shown for a $z' = 25.2$ source lying at $I - z' = 0.2$ and $V - I = 1.8$, typical of the location from which galaxies might scatter into regions of the color-color space and be misidentified as high redshift objects. The one spectroscopically identified $z = 5.19$ source is shown with a large solid square. The dashed (dot-dashed) curve shows the quasar (blue galaxy) track with redshift. Redshifts are given at the positions of the diamonds on the tracks.

3.2. Optically Faint Sample

Of the 500 X-ray sources in our sample, 77 have $z' > 25.2$. Two of these have spectroscopic redshifts ($z = 3.40$ and $z = 4.14$) from Barger et al. (2002). Of the remainder, 44 are detected above the 2σ level in V or B and cannot lie at $z > 5$, leaving 31 faint sources that could be at $z > 5$. Many of these faint sources may lie at lower redshifts (e.g., Yan et al. 2002), and some may be false X-ray detections; about half lie within a factor of 2 of the flux limit at their off-axis radius, so this is an upper bound. Within a $6'$ off-axis radius where the sensitivity is relatively uniform, 9 of these optically faint sources could have rest-frame 2–8 keV luminosities in excess of $10^{43} \text{ erg s}^{-1}$, if they were placed in the $z = 5 - 6.5$ redshift range. Only 7 of these are not detected in R or I and could lie beyond $z' = 25.2$ is $\sim 1.2 \times 10^5 \text{ deg}^{-2}$, so we expect that about 30 of our sources with bright optical identifications may

be chance projections, with the true optical counterparts being fainter. If we assume that these 30 sources are similar to the 77 isolated faint sources discussed above, then we can include these sources in our candidate $z > 5$ population with a scaling factor of 1.4.

Haiman & Loeb (1999) predicted a surface density of $\sim 50 \text{ } z > 5$ sources in a $6'$ radius circle above a flux of $2 \times 10^{-16} \text{ erg cm}^{-2} \text{ s}^{-1}$ (observed 0.4–6 keV). We find less than four such $z > 5$ objects, or a maximum of 5.6 if we use the 1.4 scale factor discussed above. The surface density is at least an order of magnitude lower than the Haiman & Loeb estimate, strengthening the similar conclusion reached by Alexander et al. (2001) and Hasinger (2002) by about a factor of three.

4. DISCUSSION

We compute the number density of $z = 5 - 6.5$ sources in the rest-frame 2–8 keV luminosity range 10^{43} to $10^{44} \text{ erg s}^{-1}$ following the procedures described in Cowie et al. (2002b). In Fig. 4a we show the number density obtained using only the one $z > 5$ spectroscopic identification (solid diamond). We also computed an upper limit to this number density by assigning all the optically faint sources that could lie in the redshift interval redshifts at the center of the interval; the horizontal bar corresponds to those with L_x in the specified luminosity range. In Fig. 4a we compare our $z = 5 - 6.5$ number density with the lower redshift number densities from Cowie et al. (2002b) for both the 10^{43} to $10^{44} \text{ erg s}^{-1}$ (solid circles) and 10^{44} to $10^{45} \text{ erg s}^{-1}$ ranges (open circles). Again, the symbols denote the number densities obtained from only the spectroscopically identified AGN, while the horizontal bars show the upper limits. The bars are not consistent with one another because all the unidentified sources are included in each redshift bin if they lie in the specified luminosity range. To compare with the optically-selected samples of Boyle et al. (2000) and Fan et al. (2001b), in Fig. 4b we show the results for an $\Omega_M = 1$, $\Omega_\Lambda = 0$ cosmology with $H_0 = 50 \text{ km s}^{-1} \text{ Mpc}^{-1}$. The small number uncertainties are large in Fig. 4, but the number densities in the 10^{43} to $10^{44} \text{ erg s}^{-1}$ range (AGN whose luminosities would classify them as Seyferts) show a slow decrease with increasing redshift from $z = 0$ to $z = 6$. This result holds even within the systematic uncertainties shown by the the horizontal bars. In contrast, the number densities in the 10^{44} to $10^{45} \text{ erg s}^{-1}$ range (AGN with quasar luminosities) peak at $z = 1.5 - 3$ and closely match in shape the evolution of the optically-selected samples. Figures 4a and b show that this conclusion does not depend on the cosmological geometry.

The number density at $z = 5 - 6.5$ for $L_x \approx 10^{43}$ to $10^{44} \text{ erg s}^{-1}$ is about three orders of magnitude higher than the optically-selected SDSS sample at $L_x \approx 10^{45} \text{ erg s}^{-1}$. While this conclusion is based on the single $z > 5$ object, the fact that other high-redshift AGN have also been found in the relatively small *Chandra* fields (Silverman et al. 2002; $z = 4.93$) and in the small (74 arcmin^2) optical field of Stern et al. (2000; $z = 5.5$) gives us confidence that the CDF-N field is not anomalous. If we use our spectroscopically identified point, the slope β of the LF ($\phi(L)dL = L^{-\beta}dL$) would be about 2.6, which is similar to the bright end slope at lower redshifts in both the optical (Pei 1995) and X-ray (Miyaji et al. 2000). If we include

the unidentified objects, the maximum value of β would be about 3. A detailed LF determination for this redshift interval will require much larger area X-ray samples.

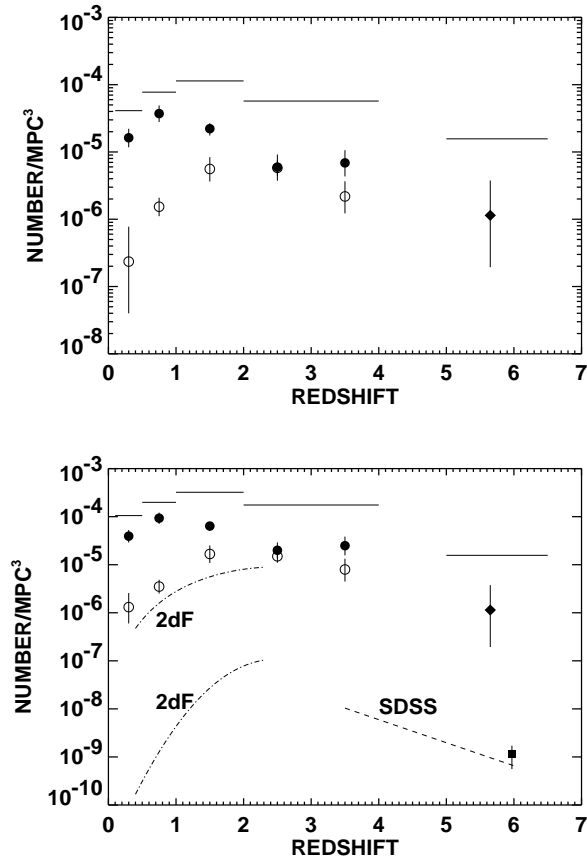


FIG. 4.— (a) Number density of sources with rest-frame 2–8 keV luminosities between 10^{43} and 10^{44} erg s $^{-1}$ (solid symbols) and between 10^{44} and 10^{45} erg s $^{-1}$ (open symbols) versus redshift. Diamond is from this paper, and circles are from Cowie et al. (2002b). Points below (above) $z = 2$ were determined from the observed-frame 2–8 keV (0.5–2 keV) sample. An intrinsic $\Gamma = 1.8$ was assumed, for which there is only a small differential K -correction to correct to rest-frame 2–8 keV. Poissonian 1σ uncertainties are based on the number of sources in each redshift interval. Horizontal bars show the maximal LF in the 10^{43} to 10^{44} erg s $^{-1}$ range found by assigning all the sources that could lie in each redshift (and then luminosity) interval a redshift at the center of the interval. (b) As in (a) but for an $\Omega_M = 1$, $\Omega_\Lambda = 0$ cosmology with $H_0 = 50$ km s $^{-1}$ Mpc $^{-1}$. Dot-dashed curves show the 2dF quasar LF of Boyle et al. (2000): upper curve is for objects with absolute 1450 Å magnitudes brighter than -23 (quasars) that roughly matches our $L_x > 10^{44}$ erg s $^{-1}$ selection, lower curve is for objects brighter than -26.8 that matches the SDSS sensitivity to high-redshift quasars. Dashed line shows the SDSS objects brighter than -26.8 in the $z = 3.5$ to $z = 6$ range. Solid square and uncertainty is for the SDSS $z > 5.7$ quasar sample to -26.8 (Fan et al. 2001b).

Fan et al. (2001b) investigated the AGN ionizing flux by fitting a variety of power-laws to extrapolate the bright SDSS data. A power-law with our observed slope of $\beta = 2.6$ matched to the SDSS data fails by more than an order of magnitude to ionize the intergalactic medium at these high redshifts, even extrapolating to faint magnitudes (their Fig. 10). We may derive this result more directly by calculating the number of ionizing photons (n_i) per baryon (n_b) produced in the redshift interval by the observed AGN. We first sum the K -corrected fluxes of the sources to determine the rest-frame 1450 Å background light they produce and then convert this to the number density of ionizing photons using the form of the near-ultraviolet AGN spectrum given in Madau, Haardt, & Rees (1999), which gives a ratio $\eta = 4.7 \times 10^{25}$ ionizing photons per erg Hz $^{-1}$ at 1450 Å. (η would be less for a galaxy shaped spectrum.) We therefore have

$$\frac{n_i}{n_b} = \frac{4 \pi \eta}{c A n_b} \sum_i f_i. \quad (2)$$

The f_i are the fluxes corresponding to the z' magnitudes for $z \sim 5.7$, and A is the observed solid angle in steradians; we set $n_b = 2.0 \times 10^{-7}$ cm $^{-3}$. In the central 6' of the CDF-N field, which has the deepest uniform sensitivity and where the $z = 5.19$ source is found, we obtain $n_i/n_b \approx 0.07$. There is almost no change if we include all the possible $z' > 25.2$ sources in the region because these objects are extremely faint in z' and hence contribute little to the sum in Eq. 2. For a Poisson distribution there is less than a 2% probability of seeing 0 or 1 sources when the true value is greater than 6, so at 98% confidence we can conclude that $n_i/n_b < 0.4$. Thus, there are too few moderate luminosity AGN at $z = 5 - 6.5$ to ionize the intergalactic medium.

Support came from the University of Wisconsin Research Committee (A.J.B.), the Alfred P. Sloan Foundation (A.J.B.), NSF grants AST-0084847 (A.J.B.), AST-0084816 (L.L.C.), and AST-9983783 (D.M.A., W.N.B.), NASA grants DF1-2001X (L.L.C.) and NAS 8-01128 (G.P.G.), and CXC grant G02-3187A (D.M.A., F.E.B., W.N.B.).

REFERENCES

- Alexander, D. M., Brandt, W. N., Hornschemeier, A. E., Garmire, G. P., Schneider, D. P., Bauer, F. E., & Griffiths, R. E. 2001, *AJ*, 122, 2156
- Barger, A. J., Cowie, L. L., Brandt, W. N., Capak, P., Garmire, G. P., Hornschemeier, A. E., Steffen, A. T., & Wehner, E. H. 2002, *AJ*, 124, 1839
- Becker, R. H., et al. 2001, *AJ*, 122, 2850
- Boyle, B. J., Shanks, T., Croom, S. M., Smith, R. J., Miller, L., Loaring, N., & Heymans, C. 2000, *MNRAS*, 317, 1014
- Brandt, W. N., et al. 2002, *ApJ*, 569, L5
- Cowie, L. L., Garmire, G. P., Bautz, M. W., Barger, A. J., Brandt, W. N., & Hornschemeier, A. E. 2002a, *ApJ*, 566, L5
- Cowie, L. L., Barger, A. J., Bautz, M. W., Brandt, W. N., & Garmire, G. P. 2002b, *ApJ*, submitted
- Fan, X., et al. 2001a, *AJ*, 122, 2833
- Fan, X., et al. 2001b, *AJ*, 121, 54
- Green, P. J., et al. 1995, *ApJ*, 450, 51
- Haehnel, M. G., Natarajan, P., & Rees, M. J. 1998, *MNRAS*, 300, 817
- Haiman, Z. & Loeb, A. 1998, *ApJ*, 503, 505
- Haiman, Z. & Loeb, A. 1999, *ApJ*, 521, L9

- Hasinger, G. 2002, in *New Visions of the X-ray Universe in the XMM-Newton and Chandra Era*, ed. F. Jansen (Noordwijk: ESA), in press
- Hornschemeier, A. E., et al. 2002, *ApJ*, submitted
- Madau, P., Haardt, F. & Rees, M. J. 1999, *ApJ*, 514, 648
- Mathur, S., Wilkes, B. J., & Ghosh, H. 2002 *ApJ*, 570, L5
- Miyaji, T., Hasinger, G., & Schmidt, M. 2000, *A&A*, 353, 25
- Miyazaki, S., et al. 2002, *PASJ*, in press
- Pei, Y.C. 1995, *ApJ*, 438, 623
- Silverman, J. D., et al. 2002, *ApJ*, 569, L1
- Songaila, A. & Cowie, L. L. 2002, *AJ*, 123, 2183
- Stern, D., Spinrad, H., Eisenhardt, P., Bunker, A. J., Dawson, S., Stanford, S. A., & Elston, R. 2000, *ApJ*, 533, L75
- Vanden Berk, D.E., et al. 2001, *AJ*, 122, 549
- Vignali, C., Brandt, W. N., & Schneider, D. P. 2003, *AJ*, in press (astro-ph/0211125)
- Yan, H., Windhorst, R. A., Odewahn, S. C., Cohen, S. H., Rottgering, H. J. A., & Keel, W. C. 2002, *ApJ*, in press (astro-ph/0208080)